Process Dynamics, Modelling and Control
CE20236
Semester 2 Coursework

A Simplified Dynamic Model of the Human Digestive System

UNIVERSITY OF BATH

Candidate number:

11017

Introduction

Obesity is an increasingly pressing issue within the UK. In order to help combat the problems it creates engineers need to utilise the technology around process dynamics, modelling and control, to gain a better understanding of the way humans process food. In this project a simplified model of the digestive system, including the stomach and the small intestine was created. This would help investigate the temperature and concentration of the process for the chosen substances of starch and glucose. The stomach is treated as a CSTR, and the small intestine is treated as a series of CSTRs, where both systems will provide steady conditions for the breakdown of food. The purpose of the model is to observe the behaviour of consumption of starch and glucose.

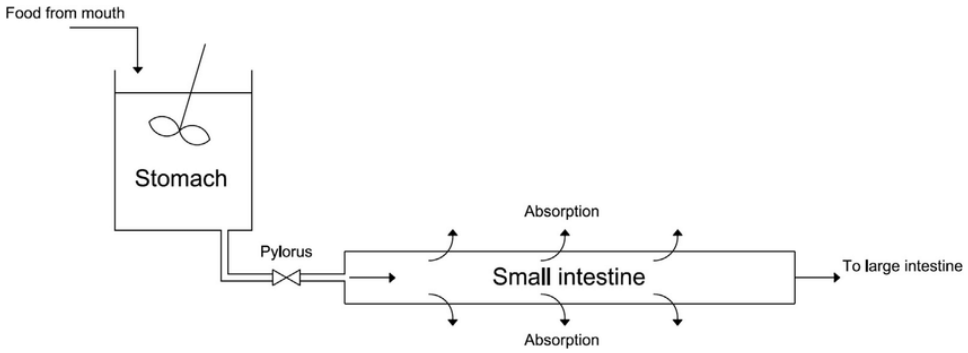

Assumptions made around the stomach

- The volume of the reaction in the stomach constant. The stomach stretches to it's maximum volume, which is 75 times its empty volume. Therefore, the volume used for stomach calculations remains unchanged.
- The mixture entering and leaving the process is perfectly mixed. The Stomach modelled as a CSTR, has perfectly mixed influent and effluent feeds. This allows for calculation of the concentration.
- The reaction is exothermic, irreversible and 1st order.
- The flowrate into and out of the stomach is constant. Although in reality the flowrate would change within the stomach, for the sake of simplicity we chose to ignore this.
- All reactions take place in the stomach, this means that there is no reaction in the small intestine.
- The only input to the stomach is pure starch. This means that during calculations, the properties used would only be for native potato starch. The other substances consumed can be ignored.
- Starch only breaks down into glucose and the rate of starch being broken down is equal to the rate of the glucose being produced.
- Starch is not generated throughout the process.
- Starch and glucose have similar properties to water at the given temperature.
- The process is an enzymatic based rate reaction so thus the Michaelis Menten equation can be used to model the rate.

Assumptions made around the stomach specifically for the Energy Balance

- The reaction is non isothermal in the stomach, so an energy balance can be used. This considers the energy input and output of a process, in this case being the total energy equalling the kinetic, potential and internal energy.
- The kinetic and potential energy can be treated as negligible, due to the assumptions that the shaft work in the stomach CSTR is zero, and that the height of liquid in the reactor remains constant.
- The surface area of heat exchange is constant, it is the total interior surface area of the stomach. The overall heat transfer coefficient is also constant; thus UA is constant.
- The feed temperature is constant. In this case, the feed temperature is the temperature of the starch stream entering the stomach.
- Blood acts like a heat jacket and regulates the temperature of the stomach.
- The density of starch remains constant because the temperature is regulated.

- The heat capacities of the products and reactants are similar and constant. We can assume this would be the heat capacity of native potato starch.

Assumptions made around the small intestine

- The thermoregulatory control off the small intestine prevents temperature change, so the small intestine is isothermal, thus no energy balance is required for that section. There is no reaction in the small intestine, so no exothermal heat is given off. Absorption is assumed to not change the temperature of the small intestine.
- Absorption in the small intestine can be modelled with Fick's law. Fick's law is applied to systems where the influent flux is the same as the effluent flux, which would be the assumptions in this case.
- Before the small intestine the 100% of the starch is converted into glucose. So only glucose is dealt with in the small intestine.
- There is a constant rate of absorption down the small intestine, so both the mass and the volumetrics flowrates can be assumed to be the same in and out of the stomach.
- The small intestine is assumed to be the shape of a tube, so the volume can easily be calculated.

Table of relevant parameters

Parameter	Value	Unit	Citation
$V_{Stomach}$	0.004	m^3	(Lumenlearning, 2017)
$F_{Stomach}$	0.0001476	$\frac{m^3}{h}$	(Biogearsengine.com, 2016)
$C_{A,in}$	12.25	$\frac{mol}{m^3}$	
$K_{m,\ Starch}$	8.634	$\frac{mol}{m^3}$	(Heitmann, Wenzig and Mersmann, 1997)
V_{max}	35.388	$\frac{mol}{m^3 h}$	
ρ_{Starch}	1450	$\frac{kg}{m^3}$	(Dengate, Baruch and Meredith, 1978)
$\Delta H_{Reaction}$	1062	$\frac{KJ}{mol}$	(Hall, 2012)
U	4.7		(de Dear et al., 1997)
$A_{Stomach}$	0.08	m^2	(Gastrointestinal tract Part 3: the stomach, 2006)
$C_{p,Starch}$	1638	$\frac{kJ}{Kg^oC}$	(Mariam, Cho and Rizvi, 2008)
$V_{Small\ Intestine}$	0.0098	m^3	
$F_{Small\ Intestine}$	0.0012	$\frac{m^3}{hour}$	(Fine et al, 1995)
$D_{Small\ Intestine}$	10^{-6}	$\frac{m^2}{hour}$	(Armen, Gharibans and Kim, 2012)
$A_{Small\ intestine}$	250	m^2	(Children's Hospital of Pittsburgh, n.d)

The volume of the stomach can stretch to hold as much as 4 litres of food, this is 75 times the empty volume (Lumenlearning, 2017), in this case we are assuming that the scenario is based on if the subject has just consumed the meal, so the stomach has stretched to the maximum size. After meals, the flowrate rises to 0.0001476 $\frac{m^3}{hour}$ through the stomach (Biogearsengine.com, 2016) and 0.0012 $\frac{m^3}{hour}$ through the small intestine (Fine et al, 1995).

In this scenario, the subject is eating 3 potatoes for their dinner. The starch content of a potato can vary, but generally a fresh potato contains 20% dry matter and 70% of this dry matter is starch. If the

average weight of a potato is 200 grams, then this means 28g of the potato is starch. Hence for a dinner of 3 potatoes, the subject consumes 84g of starch. The MR of starch is 162.14 g/mol. So, the moles of starch the subject consumed at dinner is $\frac{8}{162.14} = 0.049$ moles. With the volume of 0.004 m^3, the inlet concentration ($C_{A,in}$) is 12.25 $\frac{mol}{m^3}$. The specific type of starch used was native potato starch, so all the specific parameters such as K_m and ρ were researched.

The small intestine is assumed to be a shape of a tube, the inner radius is 0.025 m and the length is 5m (Helander and Fändriks, 2014). Hence the volume will be $\pi \times 0.025^2 \times 5 = 0.0098\ m^3$.

Transient model to mimic digestion in Stomach

The 3 potatoes that the subject consumes as their meal travels from the mouth, through the oesophagus and into the stomach. In this model, under the assumptions that have been made the only input into the stomach is starch. The glands in the stomach lining produce both stomach acid and enzymes that breakdown this starch, to provide the body with energy. During digestion muscles push food through the stomach and out of the duodenum (a short tube at the base of the stomach which leads to the small intestine) (University Hospitals, 2018).

The general mole balance of starch in the stomach is given by:

$$\text{Accumulation} = \text{In- Out + Generation – Consumption}$$

$$\frac{dm}{dt} = \dot{m}_{in} - \dot{m}_{out} - r_A$$

In this scenario the flowrate into and out of the stomach is constant and starch is not generated in the process. The change in mass with respect to time can be substituted for concentration and volume terms. Where the subscript "$_A$" represents starch in the stomach.

$$V\ \frac{dC_A}{dt} = C_{A,in}F_{in} - C_AF - r_AV$$

The process is an enzymatic based rate reaction so thus the Michaelis Menten equation can be used to model the rate, which is substituted for r_A.

$$r_A = \frac{V_{Max}C_A}{K_m + C_A}$$

Thus, the equation is rewritten as:

$$V\ \frac{dC_A}{dt} = C_{Ain}F_{in} - C_AF - V\frac{V_{Max}C_A}{K_m + C_A}$$

The Michaelis Menten equation is not linear, so must be linearised using the Taylor series. Let $F(x) = \frac{V_{Max}C_A}{K_m + C_A}$.

$$F(x) \approx \frac{V_{Max}C_{A,S}}{K_m + C_{A,S}} + \frac{V_{Max}K_m}{K_m + (C_{A,S})^2}(C_A - C_{A,S})$$

The transient model then becomes:

$$V\ \frac{dC_A}{dt} = C_{Ain}F_{in} - C_AF - V\left[\frac{V_{Max}C_{A,S}}{K_m + C_{A,S}} + \frac{V_{Max}K_m}{(K_m + C_{A,S})^2}(C_A - C_{A,S})\right]$$

Under steady State, $\frac{dC_A}{dt} = 0$. Hence the equation becomes:

$$0 = C_{Ain}F_{in} - C_{A,S}F - V\frac{V_{Max}C_A}{K_m + C_A}$$

To get the deviation form you minus the steady state information from the transient model:

$$V\ \frac{d\hat{C}_A}{dt} = \hat{C}_{Ain}F - \hat{C}_A F - V\frac{V_{Max}C_A}{(K_m + C_A)^2}\hat{C}_A$$

Once rearranged it becomes:

$$\frac{V}{F + V\frac{V_{Max}K_m}{(K_m + C_A)^2}}\frac{d\hat{C}_A}{dt} + \hat{C}_A = \frac{F_{in}}{F + V\frac{V_{Max}K_m}{(K_m + C_A)^2}}\hat{C}_{Ain}$$

Where the volume is constant, and the reaction is irreversible and exothermic.

This is now in the general first order system of $\tau\frac{d\hat{C}_A}{dt} + \hat{C}_A = K_p\hat{C}_{Ain}$ is in the form of $\tau\frac{dy(t)}{dt} + y(t) = K_p x(t)$, Therefore:

$$\tau = \frac{V}{F + V\frac{V_{Max}K_m}{{K_m}^2}} \quad and \quad Kp = \frac{F}{F + V\frac{V_{Max}K_m}{{K_m}^2}}$$

$$\tau = \frac{0.004}{0.0001476 + 0.004\frac{35.388 \times 8.634}{8.634^2}} = 0.2405$$

$$Kp = \frac{0.0001476}{0.0001476 + 0.004\frac{35.388 \times 8.634}{8.634^2}} = 0.00887$$

Taking the Laplace of $\tau\frac{d\hat{C}_A}{dt} + \hat{C}_A = K_p\hat{C}_{Ain}$

$$\mathcal{L}[\tau\frac{d\hat{C}_A}{dt}] = \tau s\ \hat{C}_A(s)$$
$$\mathcal{L}[\hat{C}_A] = \hat{C}_A(s)$$
$$\mathcal{L}[K_p\hat{C}_{Ain}] = K_p\hat{C}_{Ain}(s)$$
$$\tau s\ \hat{C}_A(s) + \hat{C}_A(s) = K_p\hat{C}_{Ain}(s)$$
$$\hat{C}_A(s)(\tau s + 1) = K_p\hat{C}_{Ain}(s)$$

The transfer function becomes: $\hat{C}_A(s) = \hat{C}_{Ain}(s)\frac{Kp}{\tau s+1}$

Using the calculated values this becomes: $\hat{C}_A(s) = \hat{C}_{Ain}(s)\frac{0.00887}{0.2405s+1}$

<u>The general energy balance around the stomach is given by:</u>

$$E_{Total} = E_{Kinetic} + E_{GPE} + U_{Internal}$$

Under the assumptions, he kinetic and potential energy can be treated as negligible

The thermodynamic relationship between the change in internal energy and change in enthalpy can be shown by the following equation. This works due to the assumption that heat capacities of the products and reactants are similar and constant.

$$\frac{dH}{dT} = \frac{dU}{dT}$$

$where\ H\ is\ given\ by$: $H = mC_p\Delta T$
$and\ m = \rho V\ and \quad \Delta T = T - T_{ref}$ but
Hence change in enthalpy becomes:

$$\frac{dH}{dT} = \rho VC_p\frac{dT}{dt} - \rho VC_p\frac{dT_{ref}}{dt}$$

There is no change in reference temperature thus, $\frac{dT_{ref}}{dt} = 0$.

$$\frac{dH}{dT} = \rho V C_p \frac{dT}{dt}$$

The energy balance for the stomach's change in internal energy in terms of temperature is shown below:

$$\frac{dH}{dT} = Energy\ in - Energy\ out + Energy\ of\ reaction + heat\ transfer$$

$$\rho V C_p \frac{dT}{dt} = F C_p (T_f - T) + \Delta H_{reaction} r_A V + UA\,(T_C - T)$$

Rearranging this gives:

$$\frac{dT}{dt} = \frac{F(T_f - T)}{V} + \frac{\Delta H_{reaction} r_A}{\rho C_p} + \frac{UA\,(T_C - T)}{\rho V C_p}$$

Where $r_A = r_p = \frac{V_{Max} C_A}{K_m + C_A}$, this is non-linear so needs to be linearised with the Taylor expansion. Let $F(x) = \frac{V_{Max} C_A}{K_m + C_A}$.

$$F(x) \approx \frac{V_{Max} C_A}{K_m + C_A} + \frac{V_{Max} K_m}{K_m + (C_A)^2}(C_A - C_{AS})$$

Subbing this into the energy balance equation gives:

$$\frac{dT}{dt} = \frac{F(T_f - T)}{V} + \frac{\Delta H_{reaction}}{\rho C_p}\frac{V_{Max} C_A}{K_m + C_A} + \frac{V_{Max} K_m}{K_m + (C_A)^2}(C_A - C_A) + \frac{UA\,(T_C - T)}{\rho V C_p}$$

At steady state $\frac{dT}{dt} = 0$, so the equation becomes.

$$0 = \frac{F(T_{f,S} - T_S)}{V_s} + \frac{\Delta H_{reaction}}{\rho C_p}\frac{V_{Max} C_{A,S}}{K_m + C_{A,S}} + \frac{V_{Max} K_m}{K_m + (C_{A,S})^2}(C_A - C_{A,S}) + \frac{UA\,(T_{C,S} - T_S)}{\rho V C_p}$$

We assume that the initial starch concentration does not affect the reaction, after rearranging the transient form of the equation is given by:

$$\frac{d\hat{T}}{dt} = \frac{F(\hat{T}_f - \hat{T})}{V} + \frac{\Delta H_{reaction}}{\rho C_p}\frac{V_{Max}\widehat{C_A}}{K_m} + \frac{UA\,(\hat{T}_C - \hat{T})}{\rho V C_p}$$

In order to be expressed in the general model of: $\tau \frac{dy(t)}{dt} + y(t) = K_{p1} X_1(t) + K_{p2} X_2(t) + K_{p3} X_3(t)$, the expression is arranged into the following form:

$$\frac{V\rho C_p}{F\rho C_p + UA}\frac{d\hat{T}}{dt} + \hat{T} = \frac{V\Delta H_{reaction} V_{Max}}{(F\rho C_p + UA)K_m}\widehat{C_A} + \frac{F\rho C_p}{F\rho C_p + UA}\hat{T}_F + \frac{UA}{F\rho C_p + UA}\hat{T}_C$$

Where: $\tau = \frac{V\rho C_p}{F\rho C_p + UA}$, $K_{p1} = \frac{V\Delta H_{reaction} V_{Max}}{(F\rho C_p + UA)K_m}$, $K_{p2} = \frac{F\rho C_p}{F\rho C_p + UA}$ $and\ K_{p3} = \frac{UA}{F\rho C_p + UA}$

Once the values are inputted the variables are:

$$\tau = 27.07, \quad K_{p1} = 0.0496, \quad K_{p2} = 0.9989\ and\ K_{p3} = 0.00107$$

Thus, the transfer function is:

$$27.07\frac{dy(t)}{dt} + y(t) = 0.0496 X_1(t) + 0.9989 X_2(t) + 0.00107 X_3(t)$$

Transient model to mimic the small intestine

The Mass balance is given by:

Input -Output + Generation – Consumption = Accumulation

$$C_{Ain}F_{in} - C_AF + r_AV = V\,\frac{dC}{dt}$$

Under the assumptions we can use Fick's law to relate the Flux to the flowrate: $r_AV = J\,A = -D\,\frac{dC}{dx}\,A$. We assume that the flowrate in and out is constant.

$$C_{Ain}F - C_AF + -D\,\frac{dC_A}{dx}A = V\,\frac{dC_A}{dt}$$

Rearranging this into the form of $\tau\frac{dy(t)}{dt} + y(t) = K_px(t)$, Gives:

$$\frac{V}{\left(F + \frac{DA}{x}\right)}\frac{dC_A}{dt} + C_A = \frac{F}{\left(F + \frac{DA}{x}\right)}C_{Ain}$$

Where:

$$\tau = \frac{V}{\left(F + \frac{DA}{x}\right)} \quad and \;\; K_p = \frac{F}{\left(F + \frac{DA}{x}\right)}$$

$$\tau = 7.84 \;\; and \;\; K_p = 0.96$$

Taking the Laplace of $\tau\frac{d\hat{C}_A}{dt} + \hat{C}_A = K_p\hat{C}_{Ain}$.

Gives: $\hat{C}_A\,(s) = \hat{C}_{Ain}\,(s)\,\frac{Kp}{\tau s+1}$

With the values, the transfer function becomes: $\hat{C}_A(s) = \hat{C}_{Ain}(s)\frac{0.96}{7.84s+1}$

Part 2

The SIMULINK model of the system can be found in *Appendix (1)*. A step change was added to the temperature of the cooling jacket input variable. Within the step change, the step time was 6, the initial temperature was 290K and the final temperature was 291K, this produced *Graph 1* in the appendix. These input and output values were chosen because when testing the step change parameters, it was found that if a value of over 303K was chosen for the output, the temperature experienced dramatic increase, thus suggesting a run-away reaction. Those specific values were chosen but anything in the range of 290k to 300k (with the output being a minimum of 1K above the input) would have been acceptable.

Graph 1 was used to investigate how this step change would impact the effect on the temperature, from the graph the process gain, K_p *and the process time constant,* τ were calculated. Another parameter that could have been useful in other scenarios is the dead time, θ. However, it was not present in this case.

$$K_p = \frac{\Delta ouput}{\Delta input} = \frac{313.6K - 300K}{1K - 0K} = 13.61 \qquad \tau = \frac{\Delta output}{Maximum\ slops}\,\frac{313.6K - 300K}{1.693} = 8.04$$

K_p measures the magnitude of the steady state system response, it is used to describe first order systems. It shows how the process behaves in response to changing dynamics and how sensitive the process is (Control Station, 2018). A high K_p results in stronger control and a faster response. The K_p is relatively high for this scenario, considering there is no control implemented as of yet. This could be explained by how the change in input was only 1K, therefore providing a larger K_p than expected. This also shows how the system is sensitive to the step change.

τ is the time constant, it expresses the speed in which the process responds to a change. It characterises the response to a step input (Control Station, 2018). In this case the time constant is 8.04

minutes. Within industry this would be a too excessive amount of time if there was a fatal problem with the process.

The initial values for a P-only, PI and PID controllers were then calculated. As the process was a closed loop the Ziegler-Nichols method was used. On SIMULINK a proportional controller was added, and the ultimate gain, K_U was set to 1 and gradually increased. It was set to 5 because this was the point where the graph created a consistent pattern of oscillations. The ultimate period P_U, is found from the distance in between the oscillation peaks. It is the period of constant amplitude limit cycles. $P_U = 20.157 - 16.458 = 3.699$.

From these parameters we can find out the proportional controller gain (K_C), the integral time (τ_I) and the derivative time (τ_D). These are initial values that can be used to test the different controllers in the later stages.

Controller	K_C	τ_I	τ_D
P	$\frac{K_C}{2} = \frac{5}{2} = 2.5$		
PI	$\frac{K_C}{2.2} = 2.273$	$\frac{P_U}{1.2} = \frac{3.699}{1.2} = 3.08$	
PID	$\frac{K_C}{1.7} = 2.94$	$\frac{P_U}{2} = 1.85$	$\frac{P_U}{8} = 0.46$

Part 3

Within the engineering industry, process control systems are commonly used to continually regulate the behaviour of devices in a predictable manner, this is done by measuring an error signal and adjusting the system accordingly, to control the range of process parameters. With the initial values calculated in the previous part a P-only, PI and PID controllers were tested in order to evaluate the response of the closed loop system. The analysis on the effect of the different controller settings can be done with the graphs produced. Parameters such as the amplitude, stability maintenance and overshoot were examined. On SIMULINK the P-only, PI and PID control was added to the model, shown on *Appendix 2.*

Proportional only control is the simplest mode of control out of the three, the output of the proportional term is proportional to the error (National Instruments, 2019. So we expect the process variable, in this case reactor temperature to deviate significantly from the desired setpoint.

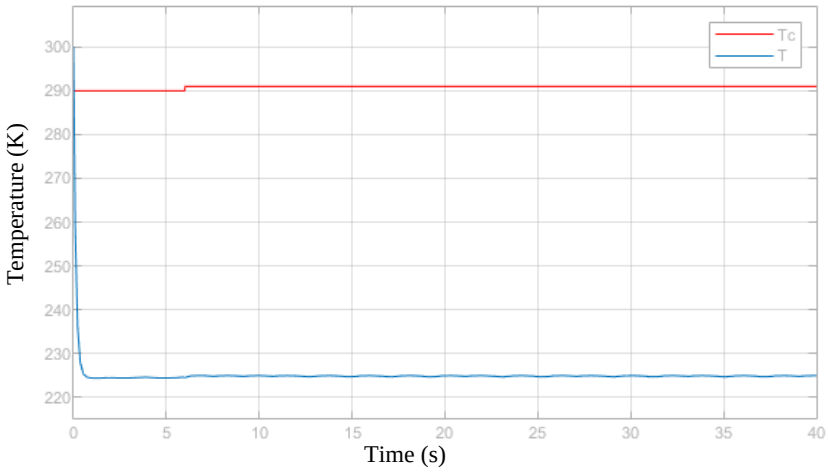

Graph 2 depicts the CSTR's cooling jacket temperature, T_C (K) and the Temperature within the reactor T (K) Against time (s).

For when the proportional band is consistently set to 2.5 and the Integral and derivative terms are set to 0.

From *Graph 2*, it can be observed that the controlled system is very far from reaching the desired set point. The reactor temperature oscillates around a specific point of roughly 225K, however this is far from the set point of 291K, thus being an ineffective form of control. This was expected, as proportional control is the simplest form of control.

Integral control is introduced to address the limitations of proportional only control, it considered both the magnetite of error as well as the length of time for which the error occurs, so should provide more control than the proportional only band. From *Graph 3*, we can immediately see that the control system stabilises around desired set point to a high degree of effectiveness and with little overshoot. The system oscillates with minimal amplitude around the setpoint, indicating that the error between the output variable and a desired set point is measured and is subsequently put through the control loop feedback to reduce the deviation between the setpoint and the output.

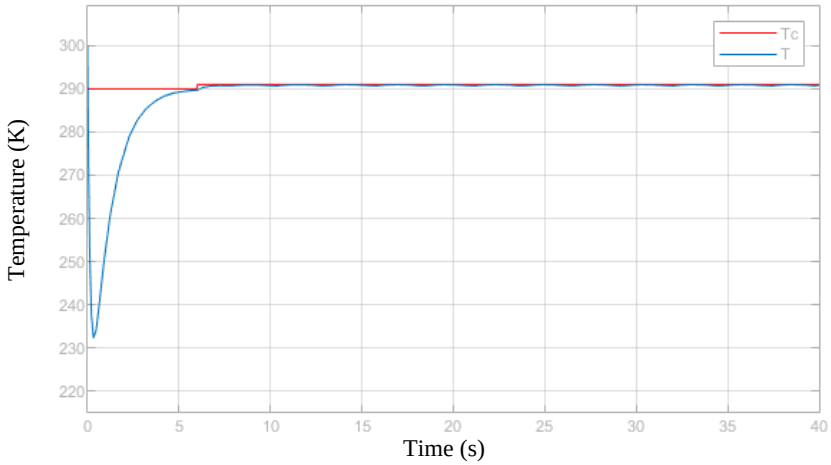

Graph 3 depicts the CSTR's cooling jacket temperature, T_C (K) and the Temperature within the reactor T (K) Against time (s) for PI control. When the proportional band is set to 2.273, the Integral term is set to 3.08 and the derivative term is set to 0.

The derivative control accounts for all the previous control features of proportional and integral but in addition to those settings, it removes the offset that is remaining. This is done by creating a signal proportional to the rate of change of the error (National Instruments, 2019).

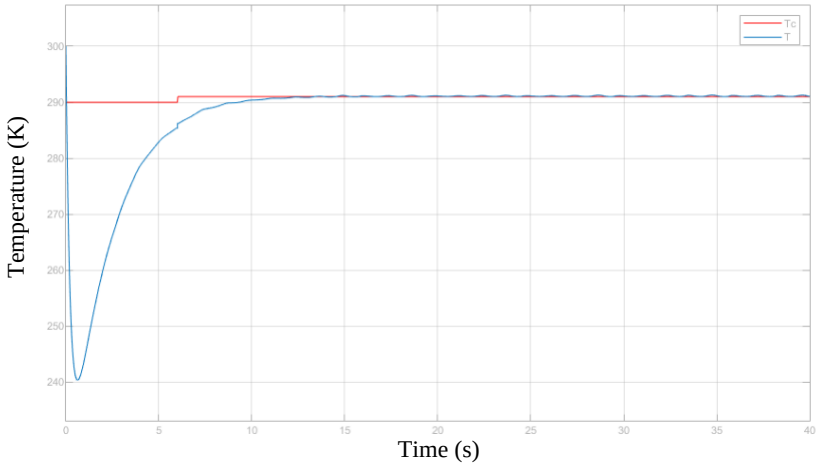

Graph 3 depicts the CSTR's cooling jacket temperature, T_C (K) and the Temperature within the reactor T (K) Against time (s). For PID control. When the proportional band is set to 2.94, the Integral term is set to 1.85 and the derivative term is set to 0.46.

The system under PID control reaches the desired set point and oscillates around it. The amplitude of the oscillations is low, but slightly larger and more frequent than when PI control was used. The system also takes slightly longer than the PI control to stabilise around the set point. However, the overshoot is low and the system does reach the setpoint. Overall, both the PI and PID controllers make quick and accurate adjustments to control the error.

In order to suggest an optimal controller, the graphs needed to undergo further analysis. The gain values of the controllers were altered to produce minimal and consistent oscillations, whilst reducing the overshoot, this was done to help with the graphical analysis. The methods of analysis chosen were finding the peak overshoot ratio, decay ratio, ITAE, IAE and ISE. *Graph 4*, shows a magnified section of the PID controller graph. The overshoot was minimal, so therefore the graph must be magnified so that visual analysis could take place.

The peak overshoot ratio is defined as the height of the first peak divided by the size of the set point change, it is an indicator of the significance of the initial oscitations. For the PID controller, the Peak overshoot ratio is calculated by:

$$\frac{initial\ overshoot}{change\ in\ set\ point} = \frac{B}{A} = \frac{291.1 - 291}{291 - 289.7} = \frac{0.1}{1.3}$$

This as a ratio is 1:13 and in percentage form is 7.7%. Amongst popular performance criteria, a peak overshoot ratio of below 10% is widely considered acceptable. The PID controller this case produces a ratio within this region, making it an effective form of controller.

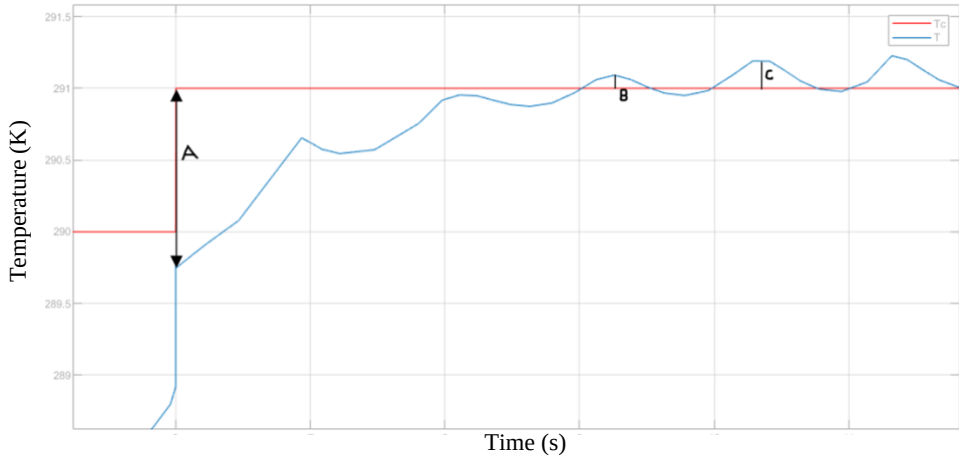

Graph 4, shows the graphical analysis of the PID control. The graph is magnified around the step point change. It shows the cooling jacket temperature, T_C (K) and the Temperature within the reactor T (K) Against time (s).

The decay ratio is calculated by: $\frac{Initial\ overshoot}{Secondary\ overshoot} = \frac{C}{B} = \frac{291.2-291}{291.1-291} = \frac{0.2}{0.1} = 2:1 = 200\%$.
In this scenario the secondary peak is larger than the initial one, thus the decay ratio is ineffective at depicting how the oscillations stabilise, hence why the ratio is over 100%.

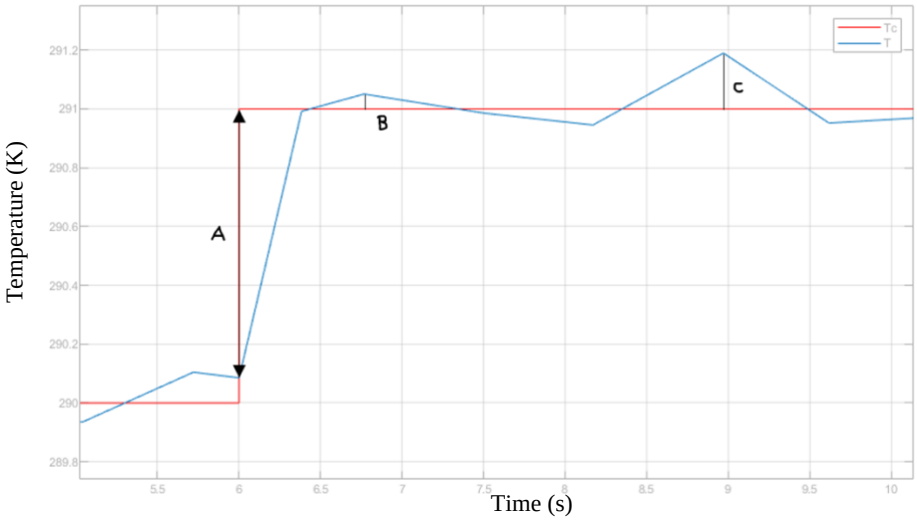

Graph 5, shows the graphical analysis of the PI control. The graph is magnified around the step point change. It shows the cooling jacket temperature, T_C (K) and the Temperature within the reactor T (K) Against time (s).

The Peak overshoot ratio is calculated by: $\frac{initial\ overshoot}{change\ in\ set\ point} = \frac{B}{A} = \frac{291.05-291}{291-290.1} = \frac{0.05}{0.9} = 1:18 = 5.556\%$. This is also less than 10% so is considered acceptable, in addition to this it is also lower than when PID control is used.
The Decay ratio is calculated by: $\frac{Initial\ overshoot}{Secondary\ overshoot} = \frac{C}{B} = \frac{291.2-291}{291.05-291} = \frac{0.2}{0.05} = 4:1 = 400\%$. This is double the value of when PID control is used. However this criteria is unreliable because the system does not initially decay, so will be ignored when choosing an optimal controller.

In the P-only control graph the measured variable does not come close to reaching the setpoint, thus there is no overshoot. So, the graphical analysis of peak overshoot ratio and decay ratio cannot be carried out.

The three error analysis: the integral of the square of the error (ISE), the integral of the absolute value of the error (IAE) and the integral of time (ITAE) were then implemented on SIMULINK, shown by *appendix 3*.

	Error analysis value		
Type of Controller	ITAE	IAE	ISE
P- only	52840	2631	173400
PI	10.49	24.66	833.1
PID	147.1	85.58	2163

Immediately it is noted that the P-only controller produces extremely high error values. This was as expected as the measured variable was not close to reaching the setpoint in the initial graph. The PI controller produced the lowest error results, indicating accuracy and precision of the system. The PID controller's values were higher than expected, considering the initial graph was similar to the PI controller's graph.

From this array of analysis, it can be seen that the optimal controller is the PI controller, It produces the lowest error values, whilst having the lowest peak overshoot ratio. To fine tune the controller, the optimal K_C was investigated. This was done by plotting K_C against the IAE.

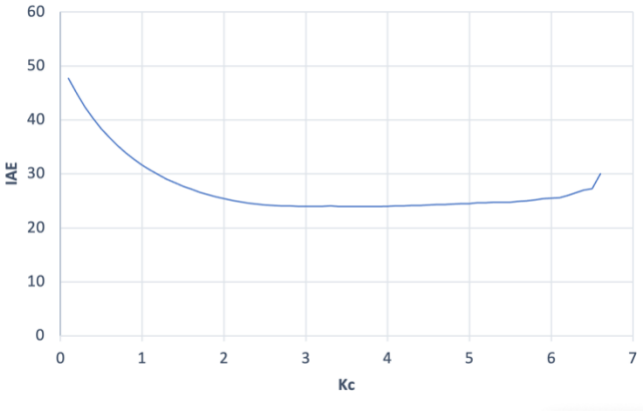

Graph 6, Shows K_C against IAE for the PI controlled system. The K_C value which produced the lowest error value was in the range of 3.4 to 4. Therefore, an optimal controller would be a PI controller with a K_C of 3.6. The values are shown on *Appendix 4.*

The final test of the optimal controller was to investigate its ability to cope with a disturbance. For this scenario, the temperature of the feed to the system was changed from 350K to 600K on SIMULINK. This was a significant change, as it was felt that the test needed to be rigours in order for it to be valid. The results are shown on *Graph 7.*

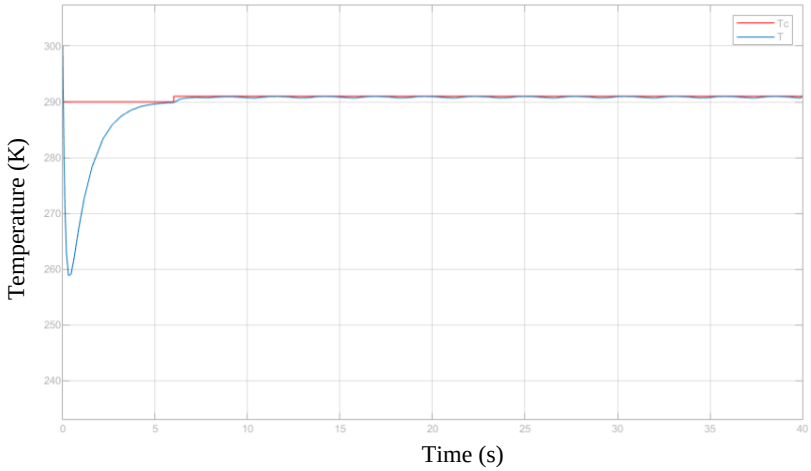

Graph 7 depicts the CSTR's cooling jacket temperature, T_C (K) and the Temperature within the reactor T (K) Against time (s) for PI control, when the disturbance is introduced.

From *Graph 7*, it is observed that the measured variable reaches the set point and oscillates with minimal amplitude around it. There is very little difference between in the graph with or without disturbance, this indicated that the control system has the ability to accurately respond to changes in the system. The small oscillations and lack of overshoot show that the PI control system is reliable when it comes to dealing with error.

References

courses.lumenlearning.com. (n.d.). *The Stomach | Biology of Aging*. [online] Available at: https://courses.lumenlearning.com/atd-herkimer-biologyofaging/chapter/the-stomach/.

Dengate, H.N., Baruch, D.W. and Meredith, P. (1978). The Density of Wheat Starch Granules: A Tracer Dilution Procedure for Determining the Density of an Immiscible Dispersed Phase. *Starch - Stärke*, 30(3), pp.80–84. doi:https://doi.org/10.1002/star.19780300304.

Fine, K.D., Santa Ana, C.A., Porter, J.L. and Fordtran, J.S. (1995). Effect of changing intestinal flow rate on a measurement of intestinal permeability. *Gastroenterology*, 108(4), pp.983–989. doi:https://doi.org/10.1016/0016-5085(95)90193-0.

Gastrointestinal tract Part 3: the stomach. (n.d.). Available at: https://cdn.ps.emap.com/wp-content/uploads/sites/3/2006/02/060221Gastrointestinal-tract.pdf.

Biogearsengine.com. (2016). Available at: https://www.biogearsengine.com/documentation/_gastrointestinal_methodology.html#:~:text=A%20static%20gastric%20secretion%20flow.

Heitmann, T., Wenzig, E. and Mersmann, A. (1997). Characterization of three different potato starches and kinetics of their enzymatic hydrolysis by an α-amylase. *Enzyme and Microbial Technology*, 20(4), pp.259–267. doi:https://doi.org/10.1016/s0141-0229(96)00121-4.

Hall, K.D., Heymsfield, S.B., Kemnitz, J.W., Klein, S., Schoeller, D.A. and Speakman, J.R. (2012). Energy balance and its components: implications for body weight regulation. *The American Journal of Clinical Nutrition*, [online] 95(4), pp.989–994. doi:https://doi.org/10.3945/ajcn.112.036350.

Mariam, I., Cho, K.Y. and Rizvi, S.S.H. (2008). Thermal Properties of Starch-Based Biodegradable Foams Produced Using Supercritical Fluid Extrusion (SCFX). *International Journal of Food Properties*, 11(2), pp.415–426. doi:https://doi.org/10.1080/10942910701444705.

Armen, A., Gharibans, Y. and Kim (2012). MODELING DIFFUSION IN THE SMALL INTESTINES. [online] Available at: https://isn.ucsd.edu/courses/beng221/problems/2012/BENG221_Project%20-%20Gharibans%20Kim.pdf.

University Hospitals (2018). *The Digestive Process: How Is Food Digested in the Stomach? | University Hospitals*. [online] Uhhospitals.org. Available at: https://www.uhhospitals.org/health-information/health-and-wellness-library/article/adult-diseases-and-conditions-v1/the-digestive-process-how-is-food-digested-in-the-stomach.

Helander, H.F. and Fändriks, L. (2014). Surface area of the digestive tract – revisited. *Scandinavian Journal of Gastroenterology*, 49(6), pp.681–689. doi:https://doi.org/10.3109/00365521.2014.898326.

Children's Hospital of Pittsburgh. (n.d.). *Differences in Small & Large Intestines | Children's Pittsburgh*. [online] Available at: https://www.chp.edu/our-services/transplant/intestine/education/about-small-large-intestines#:~:text=Looking%20at%20the%20small%20intestine.

de Dear, R.J., Arens, E., Hui, Z. and Oguro, M. (1997). Convective and radiative heat transfer coefficients for individual human body segments. *International Journal of Biometeorology*, 40(3), pp.141–156. doi:https://doi.org/10.1007/s004840050035.

Control Station. (2018). *What is Process Gain? Why is Process Gain important when tuning Processes?* [online] Available at: https://controlstation.com/blog/what-is-process-gain-why-is-process-gain-important-when-tuning-processes/.

National Instruments (2019). PID Theory Explained - National Instruments. [online] Ni.com. Available at: https://www.ni.com/en-gb/innovations/white-papers/06/pid-theory-explained.html.

Appendix

(1) Initial Simulink Model

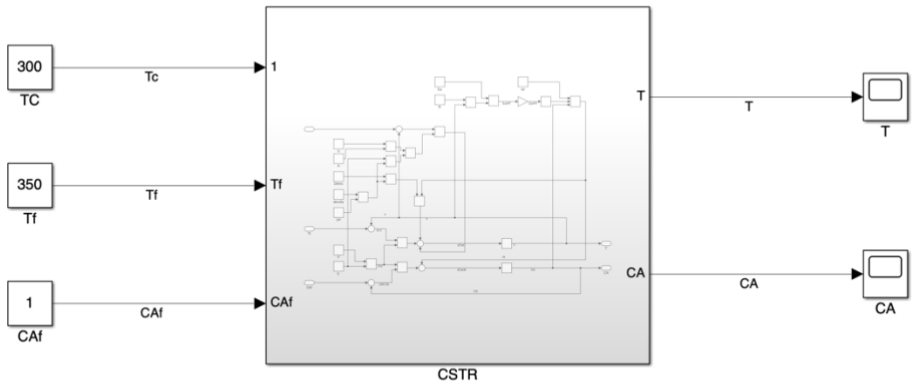

(2) Simulink Model with PID Control

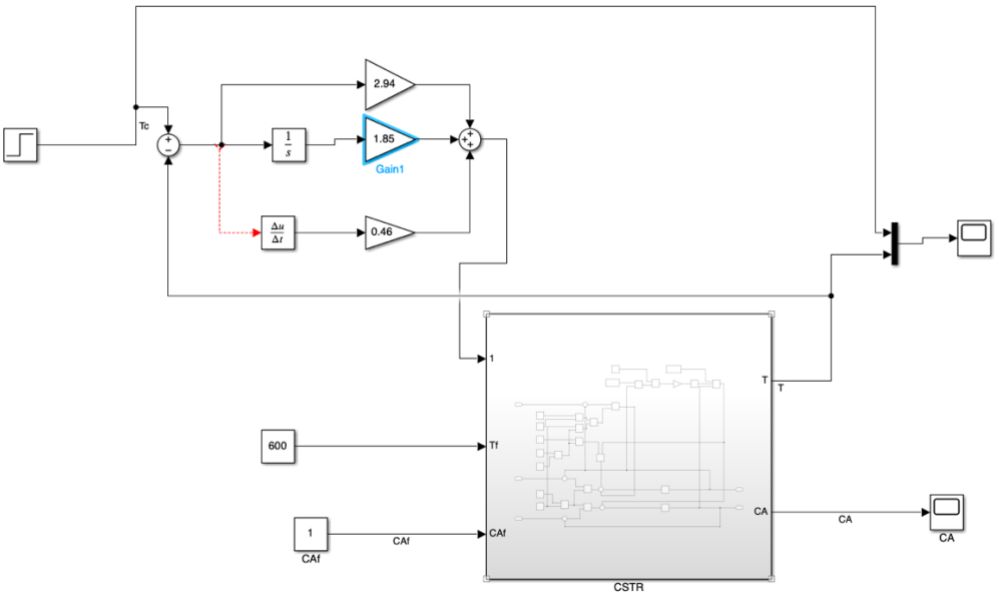

(3) *Simulink Model with PID Control and error analysis calculations*

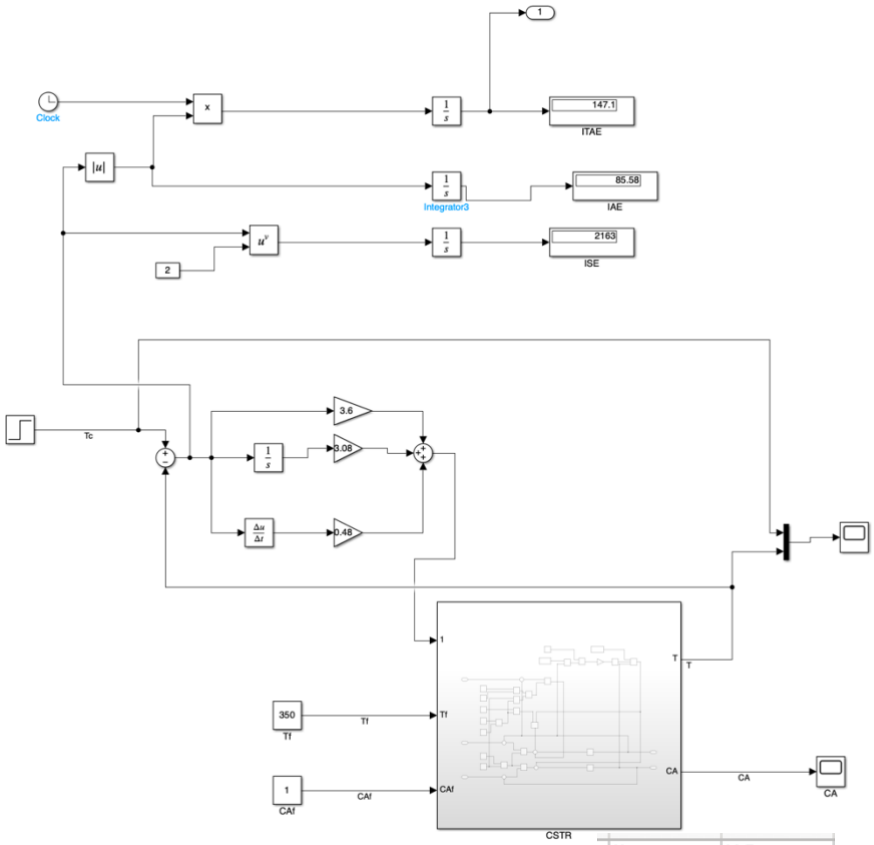

(4) SIMULINK MODEL with PID Control and error analysis calculations

Kc	IAE
0.1	47.69
0.2	44.84
0.3	42.37
0.4	40.23
0.5	38.37
0.6	36.71
0.7	35.23
0.8	33.92
0.9	32.72
1	31.65
1.1	30.7
1.2	29.83
1.3	29.06
1.4	28.34
1.5	27.72
1.6	27.15
1.7	26.63
1.8	26.17
1.9	25.77
2	25.41
2.1	25.09
2.2	24.83
2.3	24.6
2.4	24.42
2.5	24.28
2.6	24.17
2.7	24.1
2.8	24.05
2.9	24.02
3	24.02
3.1	24.01
3.2	24.01
3.3	24.1
3.4	24
3.5	24
3.6	24
3.7	24
3.8	24
3.9	24
4	24.01
4.1	24.1
4.2	24.1
4.3	24.15
4.4	24.17
4.5	24.25
4.6	24.32
4.7	24.35
4.8	24.41
4.9	24.5
5	24.54
5.1	24.67
5.2	24.7
5.3	24.73
5.4	24.76
5.5	24.8
5.6	24.9
5.7	25
5.8	25.2
5.9	25.42
6	25.49
6.1	25.6
6.2	26
6.3	26.5
6.4	27
6.5	27.3
6.6	30